



Synthesis of novel ECH crosslinked chitosan schiff base-sodium alginate for adsorption of Cd(II) ion from aqueous solution

Weili Wang^{a,*}, Qi Lu^b, Xiaoliang Ren^b, Canxiang Liu^a, Juan Jin^a, Shuyuan Yin^a, Jiming Zhang^{b,*}, Jianhua Zhou^b

^aSchool of Chemistry and Material Science, Ludong University, Yantai, 264025, China, Tel. +86 535 6672609, Fax +86 535 6696162, email: wangweilishou@163.com (W. Wang), 1369786618@qq.com (C. Liu), jinjuan8341@163.com (J. Jin), 1017059625@qq.com (S. Yin)

^bSchool of Chemistry and Pharmaceutical Engineering, Qilu University of Technology, Jinan 250353, P.R. China, Tel. +86 531 89631208, email: 13583158861@163.com (Q. Lu), laplace@163.com (X. Ren), jmzhang@yeah.net (J. Zhang), zhoujianhua4@163.com (J. Zhou)

Received 9 May 2018; Accepted 22 December 2018

ABSTRACT

A novel chitosan derivative was synthesized by crosslinking reaction of chitosan Schiff base and sodium alginate, and then used as adsorbent for Cd(II) ion. The structure of chitosan derivative was fully characterized and the adsorption behavior of Cd(II) ion was also investigated. The equilibrium and kinetic data fitted well the Langmuir and pseudo-second-order model. The estimated maximum adsorption capacity is 262.47 mg/g. Thermodynamic parameters indicates that at higher temperatures, the process is spontaneous, hence the adsorption is easy. Additionally, the regenerated adsorbent after five cycles could retain 87.15% of the adsorption capacity compared with the freshly prepared adsorbent.

Keywords: Chitosan; Sodium alginate; Adsorption; Cadmium (II) ion; Recycle

1. Introduction

Among heavy metal ions, cadmium (II) (Cd(II)) is considered to be extremely toxic for the accumulation in living organisms, bioaccumulation symptoms [1], such as kidney disease, anemia, diminish of mental capacity and renal dysfunction [2,3]. Therefore, the removal of such heavy metal ions is considered a serious issue. Many techniques have been used on heavy metal ions removal, including chemical precipitation, some electrolytic methodologies, membrane filtration and adsorption [4–8]. Within these techniques, adsorption technique has attracted great attention of researchers for its low cost, easy availability and eco-friendliness [9–11]. Several adsorbents have been developed for different metals removal from aqueous solution [12,13] or organic solvent [14,15]. For instance, some functionalized polymers, such as dendrimer-like branched polymers [16],

magnetic polymers [17,18], polyfibers [19] and silica gel composites [20] have been developed and used as adsorbents for different metal ions, furthermore, these compounds have very stable structure in solution which could be recovered and regenerated easily.

In the quest of searching an effective adsorbent for Cd(II) ion with economic performance and renewability is still of vital importance. In this regard, the utilization of biopolymers as effective adsorbents is a rising technique and is of interest in studies on the removal of heavy metal ions from aqueous solution [21,22]. Compared with other activated carbon and molecular sieve techniques, the using of biopolymers also have several advantages such as biocompatible and biodegradable [23,24]. Among biopolymers, chitosan is a natural biopolymer composed of β (1→4) linked 2-amino-2-deoxy-d-glucopyranose (N-acetylglucosamine) [25]. Chitosan is an abundant biopolymer, hence it could be

*Corresponding author.

found in the exoskeletons of insects, crustaceans and cell walls of yeast, which makes it, after cellulose, one of the richest natural polymers on the earth [26]. As a new type of renewable resource, it has many unique characteristics such as non-toxicity and antimicrobial biological activities [27]. For these reasons, chitosan has been widely investigated for adsorption of heavy metal ions in water treatment [28,29]. Such as, chitosan was grafted onto a hyperbranched polymer for Cr(VI) removal [30]. Poly(maleic acid)-grafted cross-linked chitosan microspheres was used for Cd(II) adsorption [31]. Carbon disulfide-modified magnetic ion-imprinted chitosan-Fe(III) was designed and applied for simultaneous removal of tetracycline and cadmium [32]. In despite of these advantages and studies, chitosan still have some disadvantages such as poor chemical resistance and high crystallinity, which has been a stumbling block in its appropriate use as an adsorbent [33]. To overcome the disadvantages, some kind of chitosan derivatives were developed as effective adsorbents, Li and coworkers revealed that highly cross-linked thiocarbonylchitosan gel could adsorb Cd(II) and Cr(VI) ions (81.26 and 144.68 mg/g, respectively) from aqueous solution [34], Li et al. [35] pointed out that aminothiourea chitosan strengthened magnetic biochar could be used as Cd(II) ions adsorbent for removal of cadmium(II) cations (137.3 mg/g).

Schiff base-chitosan grafted L-monoguluronic acid was used as a novel solid-phase adsorbent for the removal of congo red [36]. Chitosan–sodium alginate complexes have been used as drug delivery [37] due to their excellent properties, such as anionic, non-toxic and solubility. For sodium alginate, when the pH value increases, the –COOH group is continuously dissociated, the hydrophilicity of sodium alginate increases, and the molecular chain stretches which may make the metal adsorption easier from aqueous solution. In our present study, the modification of chitosan was achieved by crosslinking sodium alginate onto chitosan Schiff base, which was obtained from chitosan and *o*-vanillin. The resulting material (CSS/SA) has been characterized by FTIR, elemental analysis (EA), scanning electron microscope (SEM) and thermogravimetry analysis (TGA). After fully characterization, obtained CSS/SA was applied to the adsorption of Cd(II) ion from aqueous solution. The result proved that it showed high adsorption capacity for Cd(II) ion. In addition, important parameters as pH, contact time, initial concentration recycle times, isotherm and kinetic studies were also investigated.

2. Experimental

2.1. Materials and methods

Chitosan (CS) was purchased from Sinopharm Chemical Reagent Co., Ltd. China, with a weight-average molecular weight (M_w) of 4.6×10^5 and a deacetylation degree (DD) of 90%. Sodium alginate and *o*-vanillin were purchased from Aladdin Industrial Corporation, Shanghai, China. Epichlorohydrin, cadmium nitrate ($\text{Cd}(\text{NO}_3)_2 \cdot 4\text{H}_2\text{O}$), sodium hydroxide (NaOH), hydrochloric acid (HCl), methanol and ethanol were purchased from Tianjin Guan Fu Fine Chemical Research Institute, Tianjin, China. All the chemicals were of analytical grade and were used without further modification.

2.2. Characterization

Fourier transform infrared (FT-IR) spectra were recorded on a Shimadzu IR Prestige-21 infrared spectrometer using spectroscopic quality KBr powder in the range of 4000–400 cm^{-1} . Thermogravimetric analysis was conducted using a Q600 Simultaneous DSC-TGA from RT to 1000°C under N_2 at a heating rate of 10°C min^{-1} . Scanning electron microscopy (SEM) images were taken on FEI Quanta 200 field-emission scanning electron microscope. Elemental analysis was performed by an Elemental Analysensysteme Varioel (Hanau, Germany).

2.3. Synthesis of chitosan Schiff base (CSS)

Chitosan powder (1.0 g, 6.2 mmol) was dissolved in methanol (20 mL) to swell at room temperature for 1 h. Then a solution of *o*-vanillin (1.3 g, 8.54 mmol) in methanol (10 mL) was added dropwise to the reaction mixture. After refluxing for 4 h at 65°C, yellow precipitate was obtained. After filtration, the powder was washed with methanol and ethanol, extracted in a Soxhlet extractor with ethanol. Further drying under vacuum for 6 h at 50°C yields chitosan Schiff base as yellow solid. Anal. found (%): C, 55.38; H, 6.01; N, 4.08.

2.4. Synthesis of ECH crosslinked chitosan Schiff base-Sodium alginate (CSS/SA)

The CSS/SA was prepared similar to the reported procedure [36], sodium alginate (1.0 g, 4.6 mmol) was dissolved in 20 mL NaOH (0.1 M) and stirred for 12 h. After elapsed time, CSS (1.0 g) was added into the solution under stirring, 1 h later, epichlorohydrin (10 mL) was slowly added into the reaction system and then stirred at 50°C for 3 h. The mixture was filtered and washed with ethanol repeatedly. The CSS/SA was obtained after oven vacuum drying at 50°C. Anal. found (%): C, 50.36; H, 5.91; N, 2.63.

2.5. Adsorption experiments

Adsorption experiments were carried out by batch technique. To determine the optimum solution pH for Cd(II) removal, 25 mg of adsorbent was dispersed into Cd(II) solution (40 mL, 200 mg/L) in the pH range of 2–8. The solution pH was adjusted by addition of HCl (0.1 mol/L) or NaOH (0.1 mol/L). The dispersions were shaken at room temperature for 4 h. Adsorption isotherms were obtained by changing Cd(II) concentration from 50 mg L^{-1} to 300 mg L^{-1} , using Cd(II) solution (pH = 7, 40 mL) with 25 mg adsorbent. Adsorption kinetics were performed using 100 mL of Cd(II) solution (200 mg L^{-1} , pH = 7) at different time intervals with 25 mg adsorbent. To understand the effect of temperature on adsorption, experiments were carried out at temperatures ranging from 25 to 45°C. After each adsorption test, the adsorbent was separated from the solution using filter and the concentrations of Cd(II) were measured using an ICP-MS (PE-Instruments ICP-OES Optima 2000DV). All the experiments were done at least three times. The adsorption capacities (mg/g) of adsorbent were calculated as follows:

$$Q_e = V(C_0 - C_e) / M \quad (1)$$

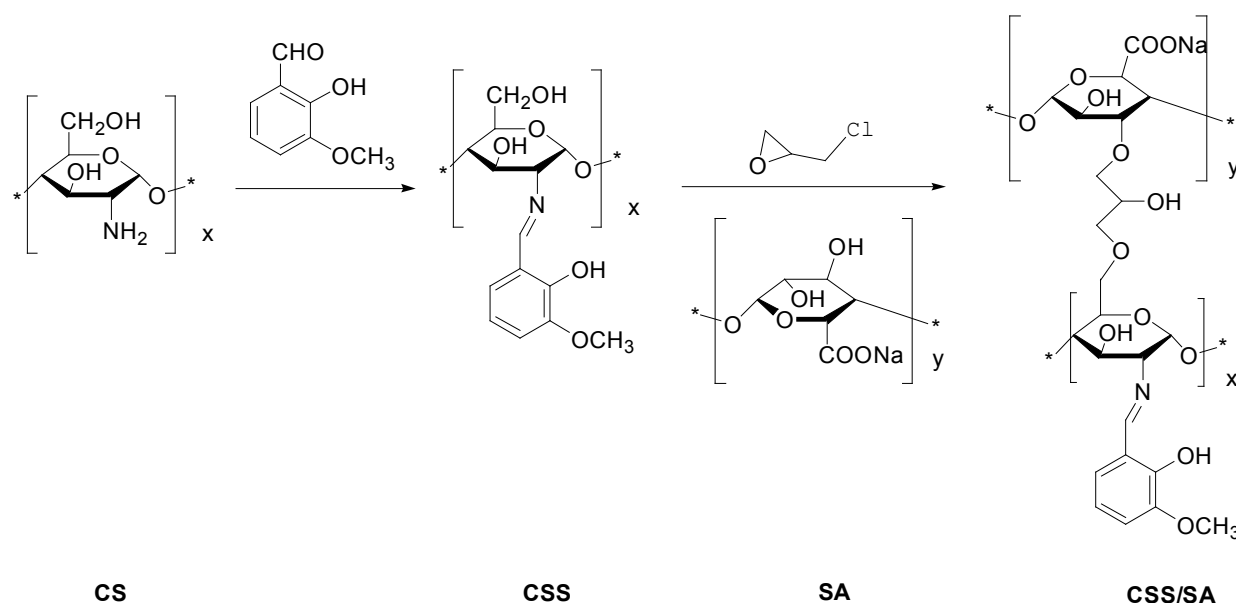


Fig. 1. Synthesis of ECH crosslinked chitosan Schiff base-Sodium alginate (CSS/SA).

where Q_e (mg/g) is the amount of Cd(II) adsorbed by the adsorbent, V (L) is the volume of the solution, C_0 (mg/L) and C_e (mg/L) are the initial and final concentrations of Cd(II), M (g) is the mass of adsorbent.

2.6. Regeneration studies

To evaluate the reusability, regeneration of the spent adsorbent was studied. 20 mg of the recovered adsorbent, which the adsorbed metal ions have been eluted from the adsorbent surface with EDTA (0.1 M), was redispersed into 40 mL of the Cd(II) solution then shaken at room temperature for 4 h. After separation, the concentration of Cd(II) was determined via ICP-MS.

3. Results and discussion

3.1. Characterization of the adsorbent

3.1.1. IR data analysis

The FTIR peaks of CS and its derivatives between 4000 and 400 cm^{-1} are shown in Fig. 2. The characteristic IR peaks of CS are: 3381 cm^{-1} (O-H stretch), 2873 cm^{-1} (C-H stretch), 1664 cm^{-1} (amide I bend), 1593 cm^{-1} (N-H bend), 1155 cm^{-1} (bridge-o stretch) and 1082 cm^{-1} (C-O stretch), which consistent with the literatures reported [38,39]. The IR spectra of the CSS, presented a strong adsorption band at 1630 cm^{-1} due to the C=N vibrations characteristic of azomethine which is not observed in chitosan. The bands at 1469 and 745 cm^{-1} are attributed to the C=C and C-H stretching in the aromatic ring, respectively [40]. These characteristic peaks also exist in CSS/SA. For the IR spectra of CSS/SA, 3200–3400 cm^{-1} shows that a broader and stronger coupling vibration, and the additional peak at 1111 cm^{-1} (-C-O-C-) becomes stronger. It could be confirmed by above arguments that proved the crosslinking occurrence.

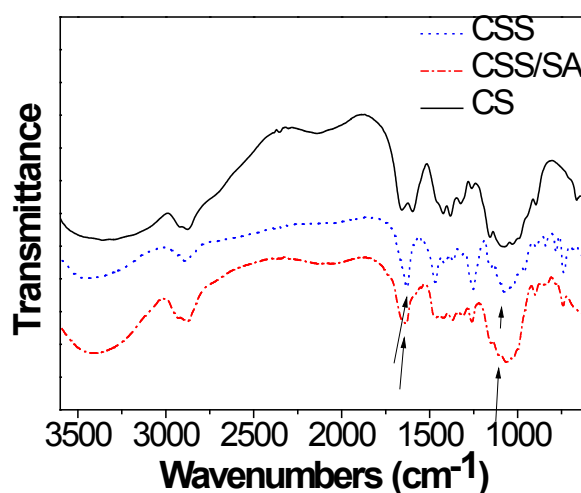


Fig. 2. IR-Spectra of CS, CSS, CSS/SA.

3.1.2. SEM analysis

The scanning electron microscopy of CS and its derivatives are shown in Fig. 3. The surface change in the SEM micrographs suggests that the structure changes before and after chitosan modification. The general morphology of CS (Fig. 3a) before modification showed a smooth surface. For Fig. 3b, the surface of CSS could be characterized as rough and folded. From Fig. 3c, the surfaces of the CSS/SA have many pores, and the pore distribution is irregular. Such pores are helpful for the mass transfer of metal ions [41].

3.1.3. TG analysis

The TG and DTG curves of CS and its derivatives are exposed in Figs. 4 and 5, respectively. From the TG-DTG

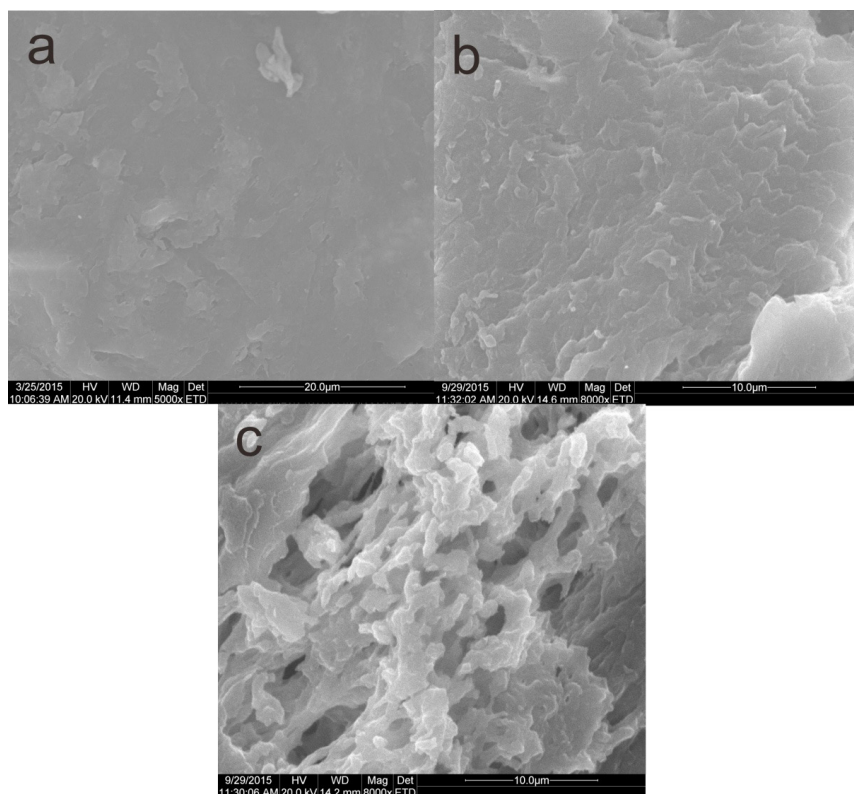


Fig. 3. The SEM images of CS(a), CSS(b), CSS/SA(c).

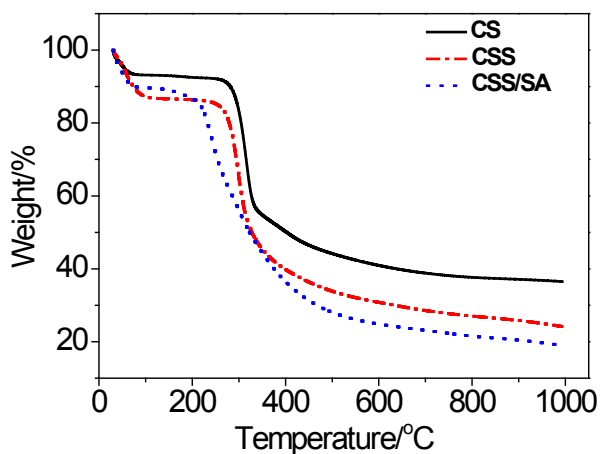


Fig. 4. TG curves of CS, CSS, CSS/SA.

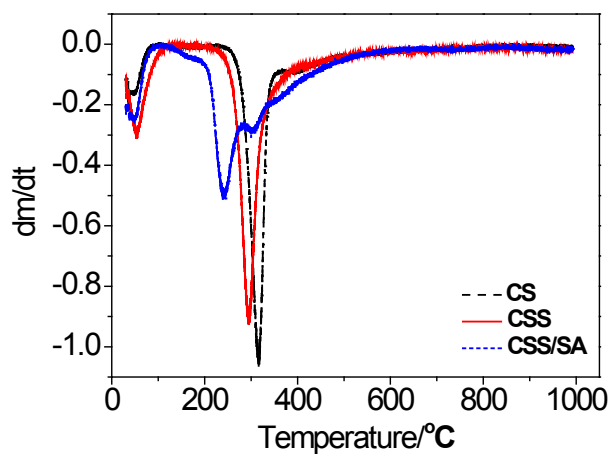


Fig. 5. DTG curves of CS, CSS, CSS/SA.

curves of all compounds, their thermal degradation stages are calculated and given in Table 1. TG-DTG curve of CS indicates that the thermal degradation takes place in three stages. In the first stage ($\sim 100^\circ\text{C}$) with a weight loss of 7.02%, this was related to the loss of physically adsorbed water molecules. In the second stage ($258^\circ\text{C}\sim 346^\circ\text{C}$) with a weight loss of 37.88% and reaches the maximum endothermic decomposition peak at 314°C , which was attributed to the decomposition of chitosan polymer. In the last stage ($346^\circ\text{C}\sim 1000^\circ\text{C}$) with a weight loss

18.64%, this was due to the decomposition of the glucosamine residual. From TG-DTG graph of CSS, it showed three different mass loss stages. First mass loss (13.61%) below 100°C may be due to the loss of surface water molecules, and the second weight loss (50.01%) could be considered to the decomposition of free chitosan unit and third degradation stage may be attributed to the decay of condensed chitosan unit. Concerning thermal stability, chitosan Schiff base is less stable than chitosan, which might be related to the decrease in the number of primary

Table 1
Thermal degradation stages of chitosan, chitosan Schiff base and CSS/SA between 0°C and 800°C

Sample	1st stage (Wt. loss, %)	2nd stage (Wt. loss, %)	3rd stage (Wt. loss, %)	Residue% (at 1000 °C)
CS	0–100 (~7.02)	258–346 (~37.88)	346–1000 (~18.64)	36.46
CSS	0–100 (~13.61)	244–458 (~50.01)	458–1000 (~25.9)	10.48
CSS/SA	0–100 (~9.64)	203–478 (~61.62)	478–1000 (~10.38)	18.36

amino groups after the chemical modification process [42]. TG-DTG curves of the CSS/SA exhibit three loses of mass during the thermal decomposition. First stages came from the loss of surface adsorbed water molecules, second one might be due to the main chains of polymer degraded seriously, and the last stage was due to the decay of the condensed chitosan unit. According to DTG curves of chitosan and its derivatives, all thermal decays are involved endothermic decomposition. However, the positions of endothermic peaks are different for different samples. Besides, the elemental analysis revealed that CSS/SA had a lower nitrogen content (2.63%) than CSS (4.08%) or CS (8.47%), the obvious decreases of nitrogen content indicates CS was successfully introduced into the CSS/SA matrix.

3.2. Adsorption behaviors

3.2.1. Effect of pH

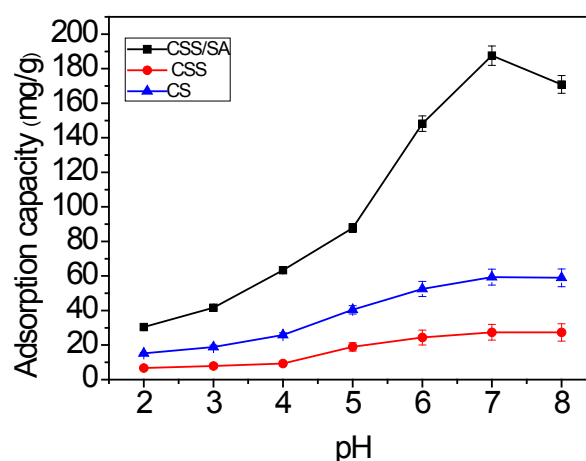
It is well known that pH has a significant influence on the adsorption process [43]. The effect of pH on the adsorption capacity of Cd(II) on the CSS/SA was observed over a pH range of 2–8 as exhibits in Fig. 6a. The adsorption capacity of Cd(II) increased markedly from pH 2–7 and decreased dramatically over pH 7. This result may be attributed to the ion-exchange interactions exist between the adsorbent and the metal ions. In acidic medium, the competition from H⁺ ions at low pH may lead to the low adsorption of metal ions, while at higher values of pH, the complexation reaction of Cd(II) with OH⁻ ions could affect the adsorption [44]. Hence, 7.0 was determined to be the optimal value of pH for the experiments.

The variation of pH before and after the addition of adsorbent in Fig. 6b proved that the adsorbent surface protonation and deprotonation process occurred during the adsorption process [36]. The introduction of *o*-vanillin and eichlorohydrin groups into the structure of CSS/SA provided plenty of functional groups, which facilitated Cd(II) adsorption.

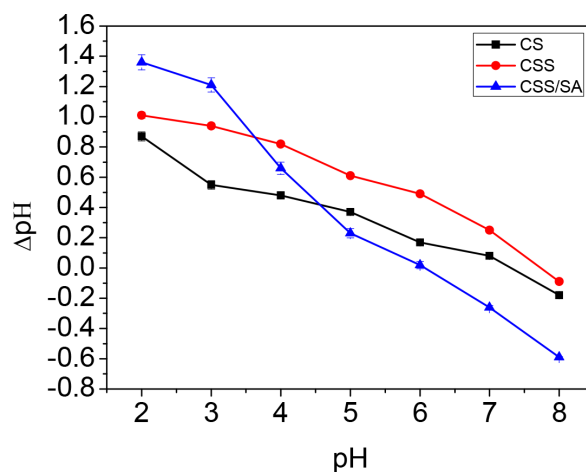
3.2.2. Adsorption isotherms

The adsorption isotherm is fundamental to understand how Cd(II) interact with adsorbents. For the adsorption isotherm studies, the initial Cd(II) concentrations are in the range of 60–200 mg L⁻¹ at room temperature (Fig. 7). The adsorption isotherms are analyzed by Langmuir and Freundlich. The mathematical form of Langmuir equation is [45]:

$$\frac{C_e}{Q_e} = \frac{C_e}{Q_{\max}} + \frac{1}{Q_{\max}b} \quad (2)$$



(a)



(b)

Fig. 6. Effect of pH value on adsorption capacity of Cd(II).

where C_e is the equilibrium concentration of the Cd(II) (mg/L), Q_e is the amount of Cd(II) adsorbed at equilibrium (mg/g), and b and Q_{\max} are the Langmuir constants, which are related to adsorption bonding energy and the maximum adsorption capacity, respectively. By linear fitting, the plot of C_e/Q_e vs. C_e indicates a straight line with high correlation coefficient ($R^2 = 0.99$) (Fig. 8a). The values of Q_m and b are calculated to be 262.47 mg/g and 0.1164 L/mg, respectively. The results indicate that the Cd(II) adsorption on CSS/SA fitted well with the Langmuir model.

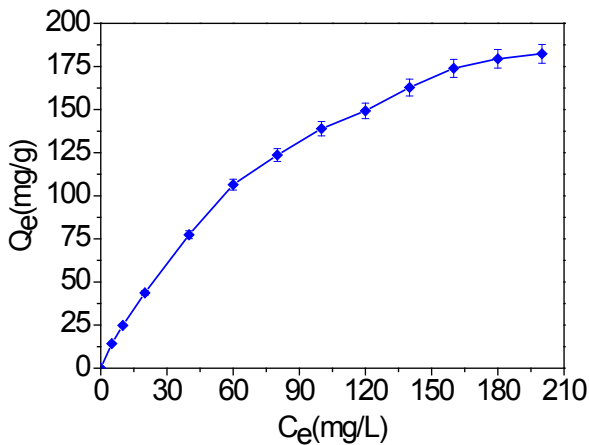


Fig. 7. The effect of initial concentration on adsorption capacity of Cd(II).

The mathematical form of Freundlich isotherm equation is [46]:

$$\ln Q_e = \ln K_F + \frac{1}{n} \ln C_e \quad (3)$$

where K_F and n are empirical constants which indicate the relative sorption capacity and sorption intensity, respectively. Q_e is defined as in equilibrium (mg/g).

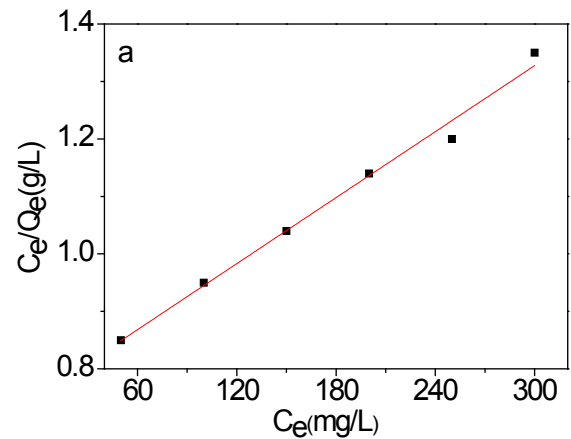
The plot of $\ln Q_e$ vs. $\ln C_e$ gives a relatively low correlation coefficient ($R^2 = 0.98$) and a n value of 2.33 by linear fitting (Fig. 8b), indicating that the adsorption of Cd(II) on CSS/SA does not preferably follow the Freundlich model. The parameters obtained from fitting the Langmuir and Freundlich models are presented and confronted in Table 2. Higher correlation coefficients indicate that Langmuir model fits the adsorption data better than Freundlich model.

Table 3 gives the adsorption capacities of some of the materials studied for the adsorptions of Cd(II) ion, including CSS/SA. CSS/SA has a relatively large adsorption capacity of 262.47 mg/g for Cd(II), illustrating that CSS/SA can be a promising material in comparison with well-known adsorbents for removal of metal ions from aqueous solutions.

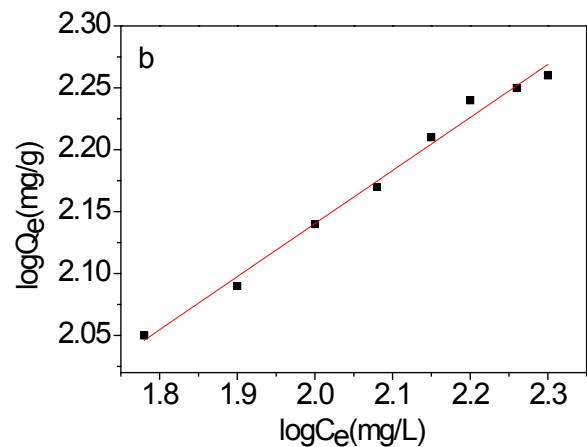
3.2.3. Adsorption kinetics

The adsorption kinetics offers useful information about the solute uptake rate and the reaction pathways [49]. The effect of contact time on the adsorption capacity of Cd(II) by CSS/SA is shown in Fig. 9. The adsorption processes were divided into two phases. The first is a fast increase phase which lasts for 180 min, and the second one is a slower stage standing for 240 min to reach equilibrium. To examine the kinetics mechanism which is attributed to direct the adsorption process, the pseudo-first-order and pseudo-second-order models were used to evaluate the experimental data. The pseudo-first-order equation (4) and the pseudo-second-order (5) are expressed as [50]:

$$\ln(Q_e - Q_t) = \ln Q_e - k_1 t \quad (4)$$



(a)



(b)

Fig. 8. Langmuir (a) and Freundlich (b) models for the adsorption of Cd(II).

$$\frac{t}{Q_t} = \frac{1}{k_2 Q_e^2} + \frac{t}{Q_e} \quad (5)$$

where Q_t (mg/g) is the amount of Cd(II) adsorbed by the adsorbent at time t (min), t is the adsorption time, k_1 (1/min) and k_2 (g/mg/min) are the rate constants for pseudo-first-order and the pseudo-second-order models, respectively. The graphs of the pseudo-first-order and the pseudo-second-order can be seen in Fig. 10, and the constant and correlation coefficients are summarized in Table 3. It was found that experimental data and the corresponding parameters calculation fits perfectly with the pseudo-second-order model.

3.2.4. Adsorption thermodynamics

The dependence of the adsorption capacity of Cd(II) with the temperature is shown in Fig. 11. The adsorption capacity of Cd(II) by CSS/SA rises up as temperature increases, indicating the adsorption reaction is endothermic.

Table 2
Constants and correlation coefficients of adsorption isotherms for adsorption Cd(II) on CSS/SA

Adsorbent	Isotherm model						
	Langmuir			Freundlich			
	Q_{max} (mg/g)	b (L/mg)	R^2	n	$1/n$	K ((mg/g/mg) ^{1/n})	R^2
CSS/SA	262.47	0.1164	0.99	2.33	0.4284	19.05	0.98

Table 3
Comparison of maximum adsorption capacities of Cd(II) on various adsorbents

Adsorbent	Adsorption capacity (mg g ⁻¹)	References
CTS-ECH-TPP	98.16	29
Nanofibrillar chitosan	60.86	44
Crab shell	154.0017	47
MMC	288.7	38
Chitosan-silica hybrid materials	73.07	39
Cr-pillared bentonite	47.55	48
CSS/SA	262.47	This work

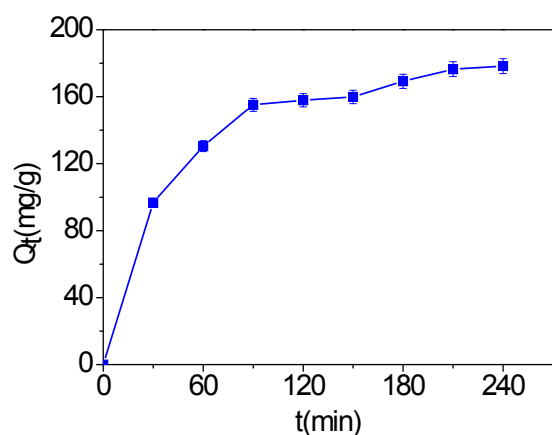


Fig. 9. The effect of contact time on adsorption capacity of Cd(II).

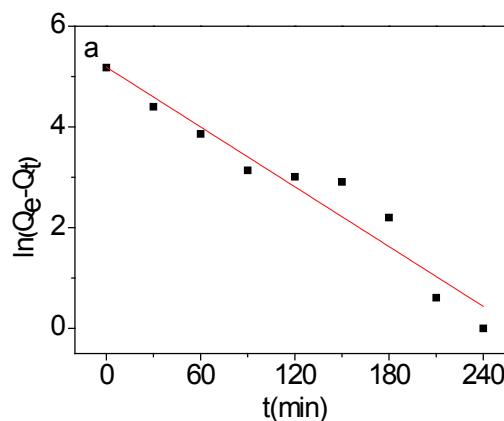
The adsorption thermodynamics parameters were calculated with equations [51]:

$$\log K_d = \Delta S^\circ / 2.303R - \Delta H^\circ / 2.303RT \quad (6)$$

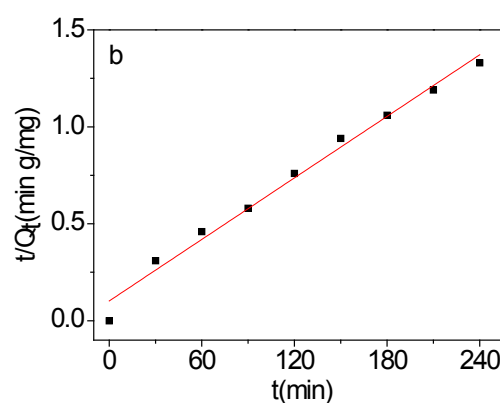
$$\Delta G^\circ = -RT \ln K_d \quad (7)$$

where R (8.314 J/mol K) is the idea gas constant, T (K) is the temperature and k (dm³/g) is the distribution coefficient of the adsorbate (Q_e/C_e), ΔG° is the Gibbs free energy change, ΔS° is the entropy change, and ΔH° is the enthalpy of adsorption process.

Fig. 12 shows the plot of $\ln K_d$ vs. $1/T$ according to Eq. (6). As shown in Table 5, the values of ΔG° are negative, which indicates Cd(II) is adsorbed by CSS/SA sponta-



(a)



(b)

Fig. 10. Pseudo-first-order (a), pseudo-second-order (b) models for the adsorption of Cd(II).

neously. Additionally, the values of ΔG° became more negative with increasing temperature, hence, the spontaneity of the Cd(II) adsorption increases with the temperature [52]. On the other hand, the positive value of ΔH° explains an endothermic of adsorption while the positive value of ΔS° indicates an increase in disorder at the adsorbent/liquid interface [53].

3.3. Reusability of the adsorbent

Regeneration and reuse of adsorbents are significant parameters from the economic point of view. Fig. 13 shows the adsorption capacity of Cd(II) after five consecutive

Table 4
Kinetic Parameters for adsorption of Cd(II) on CSS/SA

Pseudo-first-order kinetics				Pseudo-second-order kinetics		
$Q_{e,exp}$ (mg/g)	$Q_{e,cal}$ (mg/g)	k_1 (min ⁻¹)	R_1^2	$Q_{e,cal}$ (mg/g)	k_2 (g/mg/min)	R_2^2
178.3	159.47	0.0198	0.93	189.03	2.74×10^{-4}	0.99

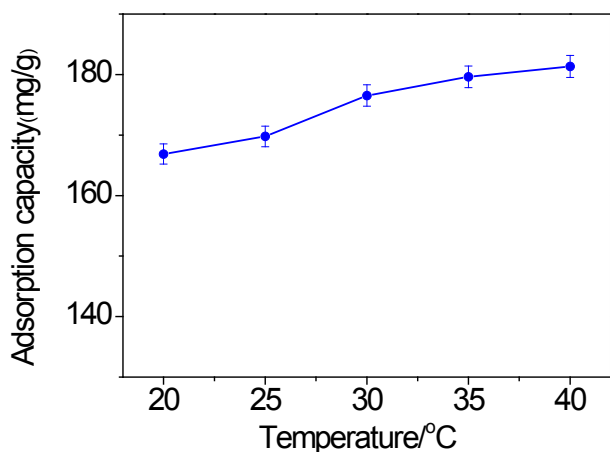


Fig. 11. The effect of temperature on adsorption capacity of Cd(II).

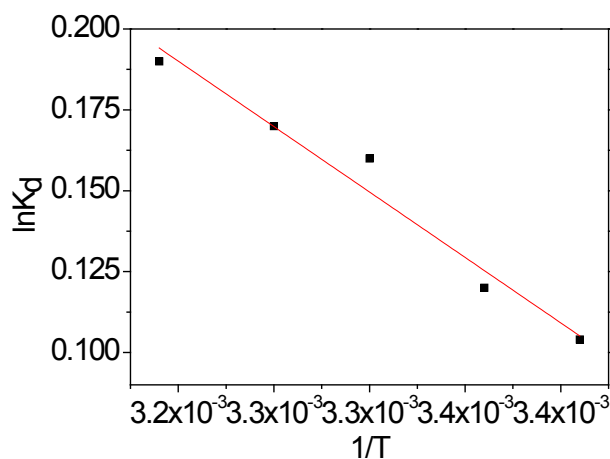


Fig. 12. Thermodynamics plots on adsorption of Cd(II).

Table 5
Thermodynamics parameters for Cd(II) on CSS/SA

Adsorbent	ΔS° (J/mol/K)	ΔH° (KJ/mol)	T (K)	ΔG° (J/mol)
CSS/SA	12.3	3.36	293	-253.34
			298	-297.31
			303	-403.06
			308	-435.32
			313	-494.43

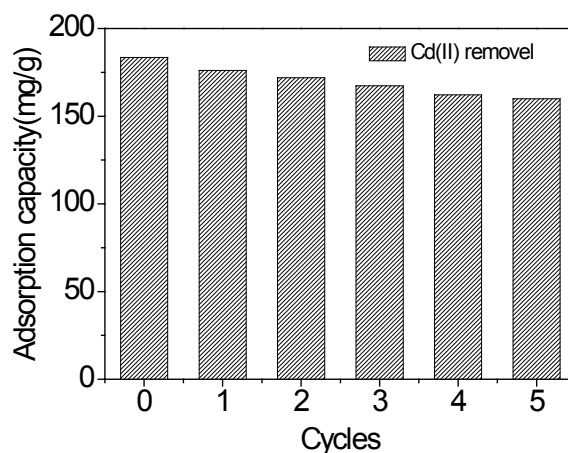


Fig. 13. Adsorption capacity of Cd(II) on CSS/SA in five cycles.

cycles. It can be clearly seen that recycled CSS/SA did not show remarkable decrease in efficiency, maintaining high adsorption capacity. However, the loaded amount of Cd(II) by regenerated CSS/SA after five cycles was 87.15% of the amount by the fresh adsorbent. The results also prove that CSS/SA could be applied in the heavy metal ions removal.

4. Conclusions

In summary, a novel chitosan derivative was synthesized from chitosan Schiff base and sodium alginate through cross-linking reaction. The CSS/SA revealed porous structure, leading to the efficient adsorption capacity of Cd(II). The maximum adsorption capacity for Cd(II) is 262.47 mg/g. The adsorption isotherms of Cd(II) followed the Langmuir adsorption isotherms, the kinetics adsorption fits the pseudo-second-order kinetic model. The positive enthalpy energy change for the adsorption process confirms the exothermic of adsorption, and a free energy change indicates the spontaneity of the process. Additionally, recycled CSS/SA still exhibits high adsorption capacity for Cd(II) even after five cycles. The high adsorption capacity, simple and convenient synthesis makes CSS/SA more competitive for removal of heavy metals from aqueous solution. This study provides an important method related to the water treatment and the environmental protection through a stable, inexpensive and recyclable bio-based adsorbent.

Acknowledgements

This work was supported by the Natural Science Foundation of Shandong Province (No. ZR2017PB006), the

Ph.D Programs Foundation of Ludong University (No. 32840301), the National University Student Innovation and entrepreneurship training Program (No. 201710451034, 201810451326, 201810451344) and the Innovation Foundation for students of Ludong University (No. ld171062).

References

- [1] D.K. Singh, S. Mishra, Synthesis, characterization and removal of Cd(II) using Cd(II)-ion imprinted polymer, *J. Hazard. Mater.*, 164 (2009) 1547–1551.
- [2] Y. Liu, L. Xu, J. Liu, X. Liu, C. Chen, G. Li, Y. Meng, Graphene oxides cross-linked with hyperbranched polyethylenimines: Preparation, characterization and their potential as recyclable and highly efficient adsorption materials for lead(II) ions, *Chem. Eng. J.*, 285 (2016) 698–708.
- [3] Y. Niu, R. Qu, H. Chen, L. Mu, X. Liu, T. Wang, Y. Zhang, C. Sun, Synthesis of silica gel supported salicylaldehyde modified PAMAM dendrimers for the effective removal of Hg(II) from aqueous solution, *J. Hazard. Mater.*, 278 (2014) 267–278.
- [4] M.M. Matlock, B.S. Howerton, D.A. Atwood, Chemical precipitation of heavy metals from acid mine drainage, *Water Res.*, 36 (2002) 4757–4764.
- [5] H. Aghayan, A.R. Khanchi, A.R. Mahjoub, Synthesis and characterization of cesium molybdo vanado phosphate immobilized on platelet SBA-15: An efficient inorganic composite ion-exchanger for gadolinium ion sorption, *Appl. Surf. Sci.*, 274 (2013) 7–14.
- [6] L. Zhang, Y.H. Zhao, R. Bai, Development of a multifunctional membrane for chromatic warning and enhanced adsorptive removal of heavy metal ions: Application to cadmium, *J. Membr. Sci.*, 379 (2011) 69–79.
- [7] C. Liu, X. Sun, L. Liu, J. Liu, M. Qi, H. An, Synthesis of 8-Hydroxyquinoline-functionalized polyglycidyl methacrylate resin and its efficient adsorption and desorption for Pb(II), *Desal. Water Treat.*, 57 (2016) 18425–18437.
- [8] Y. Niu, R. Qu, C. Sun, C. Wang, H. Chen, C. Ji, Y. Zhang, X. Shao, F. Bu, Adsorption of Pb(II) from aqueous solution by silica-gel supported hyperbranched polyamidoamine dendrimers, *J. Hazard. Mater.*, 244–245 (2013) 276–286.
- [9] X. Song, Y. Niu, P. Zhang, C. Zhang, Z. Zhang, Y. Zhu, R. Qu, Removal of Co(II) from fuel ethanol by silica-gel supported PAMAM dendrimers: Combined experimental and theoretical study, *Fuel*, 199 (2017) 91–101.
- [10] L. Guo, C. Sun, G. Li, C. Liu, C. Sun, Thermodynamics and kinetics of Zn(II) adsorption on crosslinked starch phosphates, *J. Hazard. Mater.*, 161 (2009) 510–515.
- [11] Y. Zhang, R. Qu, C. Sun, C. Sun, H. Chen, P. Yin, Improved synthesis of silica-gel-based dendrimer-like highly branched polymer as the Au(III) adsorbent, *Chem. Eng. J.*, 270 (2015) 110–121.
- [12] Y. Niu, H. Liu, R. Qu, S. Liang, H. Chen, C. Sun, and Y. Cui, Preparation and characterization of thiourea-containing silica gel hybrid materials for Hg(II) adsorption, *Ind. Eng. Chem. Res.*, 54 (2015) 1656–1664.
- [13] C. Sun, G. Zhang, C. Wang, R. Qu, Y. Zhang, Q. Gu, A resin with high adsorption selectivity for Au(III): Preparation, characterization and adsorption properties, *Chem. Eng. J.*, 172 (2011) 713–720.
- [14] F. Cao, P. Yin, X. Liu, C. Liu, R. Qu, Mercury adsorption from fuel ethanol onto phosphonated silica gel prepared by heterogeneous method, *Renew. Energy*, 71 (2014) 61–68.
- [15] C. Dong, R. Fu, C. Sun, R. Qu, C. Ji, Y. Niu, Y. Zhang, Comparison studies of adsorption properties for copper ions in fuel ethanol and aqueous solution using silica-gel functionalized with 3-amino-1,2-propanediol, *Fuel*, 226 (2018) 331–337.
- [16] X. Song, Y. Niu, Z. Qiu, Z. Zhang, Y. Zhou, J. Zhao, H. Chen, Adsorption of Hg(II) and Ag(I) from fuel ethanol by silica gel supported sulfur-containing PAMAM dendrimers: Kinetics, equilibrium and thermodynamics, *Fuel*, 206 (2017) 80–88.
- [17] S. Zhang, Y. Zhang, J. Liu, Q. Xu, H. Xiao, X. Wang, H. Xu, J. Zhou, Thiol modified Fe₃O₄/SiO₂ as a robust, high effective, and recycling magnetic sorbent for mercury removal, *Chem. Eng. J.*, 226 (2013) 30–38.
- [18] J. Zhao, Y. Niu, B. Ren, H. Chen, S. Zhang, J. Jin, Y. Zhang, Synthesis of Schiff base functionalized superparamagnetic Fe₃O₄ composites for effective removal of Pb(II) and Cd(II) from aqueous solution, *Chem. Eng. J.*, 347 (2018) 574–584.
- [19] Y. Wang, R. Qu, F. Pan, X. Jia, C. Sun, C. Ji, Y. Zhang, K. An, Y. Mu, Preparation and characterization of thiol- and amino-functionalized polysilsesquioxane coated poly(p-phenylene-terephthalamide) fibers and their adsorption properties towards Hg(II), *Chem. Eng. J.*, 317 (2017) 187–203.
- [20] P. Yin, Q. Xu, R. Qu, G. Zhao, Y. Sun, Adsorption of transition metal ions from aqueous solutions onto a novel silica gel matrix inorganic-organic composite material, *J. Hazard. Mater.*, 173 (2010) 710–716.
- [21] S. Zhang, Y. Zhang, G. Bi, J. Liu, Z. Wang, Q. Xu, H. Xu, X. Li, Mussel-inspired polydopamine biopolymer decorated with magnetic nanoparticles for multiple pollutants removal, *J. Hazard. Mater.*, 270 (2014) 27–34.
- [22] L. Guo, Y. Cao, G. Li, J. Liu, L. Han, H. Zhang, Preparation of starch sulfate resin and its adsorption performance for malachite green, *Desal. Water Treat.*, 97 (2017) 321–328.
- [23] M. Xu, P. Yin, X. Liu, X. Dong, Y. Yang, Z. Wang, R. Qu, Optimization of biosorption parameters of Hg(II) from aqueous solutions by the buckwheat hulls using response surface methodology, *Desal. Water Treat.*, 51 (2013) 4546–4555.
- [24] R. Li, J.J. Wang, L. A. Gaston, B. Zhou, M. Li, R. Xiao, Q. Wang, Z. Zhang, H. Huang, W. Liang, H. Huang, X. Zhang, An overview of carbothermal synthesis of metalebiochar composites for the removal of oxyanion contaminants from aqueous solution, *Carbon*, 129 (2018) 674–687.
- [25] C.L. Schauer, M.S. Chen, Color changes in chitosan and poly(allyl amine) films upon metal binding, *Thin Solid Films*, 434 (2003) 250–257.
- [26] M.H. Mohammed, P.A. Williams, O. Tverezovskaya, Extraction of chitin from prawn shells and conversion to low molecular mass chitosan, *Food Hydrocolloids*, 31 (2013) 166–171.
- [27] M.N. Kumar, R.A. Muzzarelli, C. Muzzarelli, Chitosan chemistry pharmaceutical perspectives, *Chem. Rev.*, 104 (2004) 6017–6084.
- [28] R. Qu, C. Sun, F. Ma, Y. Zhang, C. Ji, Q. Xu, C. Wang, H. Chen, Removal and recovery of Hg(II) from aqueous solution using chitosan-coated cotton fibers, *J. Hazard. Mater.*, 167 (2009) 717–727.
- [29] R. Laus, T.G. Costa, B. Szpoganicz, V.T. Fávere, Adsorption and desorption of Cu(II), Cd(II) and Pb(II) ions using chitosan crosslinked with epichlorohydrin-triphosphate as the adsorbent, *J. Hazard. Mater.*, 183 (2010) 233–241.
- [30] Q. Li, Bin. Xu, L. Zhuang, X. Xu, G. Wang, X. Zhang, J. Chen, Y. Tang, Preparation, characterization, adsorption kinetics and thermodynamics of chitosan adsorbent grafted with a hyperbranched polymer designed for Cr(VI) removal, *Cellulose*, 25 (2018) 1–16.
- [31] Z. Yu, Q. Dang, C. Liu, D. Cha, H. Zhang, W. Zhu, Q. Zhang, B. Fan, Preparation and characterization of poly(maleic acid)-grafted cross-linked chitosan microspheres for Cd(II) adsorption, *Carbohydr. Polym.*, 172 (2017) 28–39.
- [32] A. Chen, C. Shang, J. Shao, Y. Lin, S. Luo, J. Zhang, H. Huang, M. Lei, Q. Zeng, *Carbohydr. Polym.*, 155 (2017) 19–27.
- [33] H. Zhao, J. Xu, W. Lan, T. Wang, Microfluidic production of porous chitosan/silica hybrid microspheres and its Cu(II) adsorption performance, *Chem. Eng. J.*, 229 (2013) 82–89.
- [34] R. Li, W. Liang, M. Li, S. Jiang, H. Huang, Z. Zhang, J.J. Wang, M.K. Awasthi, Removal of Cd(II) and Cr(VI) ions by highly cross-linked Thiocarbonylchitosan gel, *Int. J. Biol. Macromol.*, 104 (2017) 1072–1081.
- [35] R. Li, W. Liang, H. Huang, S. Jiang, D. Guo, M. Li, Z. Zhang, A. Ali, J.J. Wang, *J. Applied Poly. Sci.*, 135 (2018) 46239.
- [36] B. Yuan, L. Qiu, H. Su, C. Cao, J. Jiang, Schiff base - Chitosan grafted L-mono-glucuronic acid as a novel solid-phase adsorbent for removal of congo red, *Int. J. Biol. Macromol.*, 82 (2016) 355–360.

- [37] R.C. Nagarwal, R. Kumar, J. K. Pandit, Chitosan coated sodium alginate-chitosan nanoparticles loaded with 5-FU for ocular delivery: in vitro characterization and in vivo study in rabbit eye, *Eur. J. Pharm. Sci.*, 47 (2012) 678–685.
- [38] G. Zeng, Y. Liu, L. Tang, Enhancement of Cd(II) adsorption by polyacrylic acid modified magnetic mesoporous carbon, *Chem. Eng. J.*, 259 (2015) 153–160.
- [39] E. Repo, J.K. Warchol, A. Bhatnagar, M. Sillanpää, Heavy metals adsorption by novel EDTA-modified chitosan–silica hybrid materials, *J. Colloid Interf. Sci.*, 358 (2011) 261–267.
- [40] M. Monier, D.M. Ayad, Y. Wei, A.A. Sarhan, Adsorption of Cu(II), Co(II), and Ni(II) ions by modified magnetic chitosan chelating resin, *J. Hazard. Mater.*, 177 (2010) 962–970.
- [41] C. Jeon, W.H. Holl, Chemical modification of chitosan and equilibrium study for mercury ion removal, *Water Res.*, 37 (2003) 4770–4736.
- [42] C. Demetgül, S. Serin, Synthesis and characterization of a new vic-dioxime derivative of chitosan and its transition metal complexes, *Carbohydr. Polym.*, 72 (2008) 506–512.
- [43] C. Sun, R. Qu, S. Song, H. Chen, X. Liu, C. Sun, G. Liu, Synthesis of 2-phenoxyethanol/formaldehyde copolymer beads by dispersion polycondensation and their adsorption properties for copper ions after polyamine modification, *Desal. Water Treat.*, 57 (2016) 13722–13732.
- [44] D. Liu, Z. Li, Y. Zhu, Recycled chitosan nanofibril as an effective Cu(II), Pb(II) and Cd(II) ionic chelating agent: Adsorption and desorption performance, *Carbohydr. Polym.*, 111 (2014) 469–476.
- [45] R. Qu, Y. Zhang, W. Qu, C. Sun, J. Chen, Y. Ping, H. Chen, Y. Niu, Mercury adsorption by sulfur- and amidoxime-containing bifunctional silica gel based hybrid materials, *Chem. Eng. J.*, 2013 (219) 51–61.
- [46] J. Chen, R. Qu, Y. Zhang, C. Sun, C. Wang, C. Ji, P. Yin, H. Chen, Y. Niu, Preparation of silica gel supported amidoxime adsorbents for selective adsorption of Hg(II) from aqueous solution, *Chem. Eng. J.*, 209 (2012) 235–244.
- [47] H.K. An, B.Y. Park, D.S. Kim, Crab shell for the removal of heavy metals from aqueous solution, *Water Res.*, 35 (2001) 3551–3556.
- [48] T. Fatma, Synthesis, characterization, and adsorption properties of Fe/Cr-pillared bentonites, *Ind. Eng. Chem. Res.*, 50 (2011) 7228–7240.
- [49] R. Qu, X. Sun, C. Sun, Y. Zhang, C. Wang, C. Ji, H. Chen, P. Yin, Chemical modification of waste poly(p-phenylene terephthalamide) fibers and its binding behaviors to metal ions, *Chem. Eng. J.*, 181–182 (2012) 458–466.
- [50] Y. Wang, R. Qu, F. Pan, X. Jia, C. Sun, C. Ji, Y. Zhang, K. An, Y. Mu, Preparation and characterization of thiol- and amino-functionalized polysilsesquioxane coated poly(p-phenylene terephthal amide) fibers and their adsorption properties towards Hg(II), *Chem. Eng. J.*, 317 (2017) 187–203.
- [51] I.H. Lee, Y.C. Kuan, J.M. Chern, Equilibrium and kinetics of heavy metal ion exchange, *J. Chin. Inst. Chem. Eng.*, 38 (2007) 71–84.
- [52] Z.D. Wen, D.W. Gao, Z. Li, N.Q. Ren, Effects of humic acid on phthalate adsorption to vermiculite, *Chem. Eng. J.*, 223 (2013) 298–303.
- [53] M. Bhaumik, A. Maity, V.V. Srinivasu, M.S. Onyango, Enhanced removal of Cr(VI) from aqueous solution using polypyrrole/Fe₃O₄ magnetic nanocomposite, *J. Hazard. Mater.*, 190 (2011) 381–390.